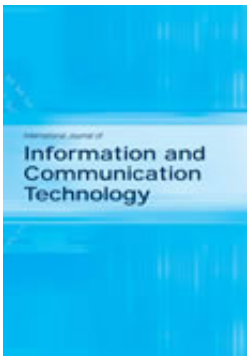

International Journal of Information and Communication Technology

ISSN online: 1741-8070 - ISSN print: 1466-6642
https://www.inderscience.com/ijict

Research on self-driving tour path planning method based on collaborative edge computing

Zhongbin Wang

DOI: 10.1504/IJICT.2023.10052209

Article History:

Received:	22 July 2020
Last revised:	15 January 2021
Accepted:	17 January 2021
Published online:	14 December 2022

Research on self-driving tour path planning method based on collaborative edge computing

Zhongbin Wang

Tibet Agriculture and Animal Husbandry University,
Nyingchi 860000, China
Email: zhongbin@mls.sinanet.com

Abstract: In order to overcome the problem of inaccurate results of traditional self-driving path planning methods, a new self-driving path planning method based on collaborative edge computing is designed and proposed. In this method, collaborative edge computing method is used to remove the abnormal data and improve the accuracy of path planning. From the point of view of optimising network performance, the objective function of network channel capacity of candidate path and the multi-objective optimisation model of path selection problem are established. Finally, the Nash negotiation axiom in game theory is combined to solve the multi-objective optimisation model to realise the self-driving travel path planning. Experimental results show that the proposed method can effectively remove abnormal data, the highest removal rate is 99.74%, and the planning efficiency is above 96%.

Keywords: collaborative edge computing; self-driving tour; abnormal data; mapping relationship; objective function.

Reference to this paper should be made as follows: Wang, Z. (2023) 'Research on self-driving tour path planning method based on collaborative edge computing', *Int. J. Information and Communication Technology*, Vol. 22, No. 1, pp.89–104.

Biographical notes: Zhongbin Wang received his Master of Science in Ecology from Tibet University in 2013. Currently, he is an Associate Professor in the College of Resources and Environment of Tibet Agriculture and Animal Husbandry University. His research interests include regional tourism planning, machine regional tourism planning, and regional tourism planning.

1 Introduction

In recent years, the number of tourists in China continues to increase. Affected by the rapid expansion of the tourism industry and the tourism market, all kinds of chaos in the tourism service market continue (Chu et al., 2018), especially during the holidays. With the rapid development of transportation infrastructure and the increasing income of residents, self-driving travel is accepted by more and more tourists. Self-driving travel does not depend on the city service market. Self-driving tour has the characteristics of autonomy, flexibility, selectivity and diversity. The path planning of self-driving tour has an important impact on the overall experience, time-consuming and cost of self-driving tour. Therefore, we should study a self-driving travel path planning method to improve the self-driving travel experience and reduce the overall cost.

In recent years, foreign scholars have studied the problem of path planning. Wei and Jin (2019) proposed a self-driving travel path planning method based on neural network Q-learning algorithm to train deep neural network in dynamic road network environment. Then the weights after training are set as the initial weights of the deep neural network in the dynamic environment, and the parameters in the dynamic environment are trained at the same time. Finally, combined with space robot, path planning is realised effectively, but this method is difficult to remove the abnormal data, resulting in the planning result is not ideal. In Feng and Yang (2019), a self-driving travel path planning method based on spatiotemporal similarity clustering is proposed. According to the fast search of the current path of the model, the initial line is obtained, and then the path is smoothed by the internal fillet method to obtain the best self-driving travel path. However, this method has the problem of high planning cost. Li and Hu (2018) propose a path planning method for self-driving travel based on RFID technology. By improving the traditional A* algorithm, the path planning task can be effectively realised, and the optimised path points can be obtained to complete the path planning for self-driving travel. However, this method has the problem of low planning efficiency.

Aiming at the problems of low efficiency and unsatisfactory planning results, a self-driving path planning method based on collaborative edge computing is proposed. The overall scheme of this method is as follows:

1 In order to improve the accuracy of self-driving tour path planning results, it is necessary to remove the abnormal data in the planning process. Therefore, the collaborative edge calculation method is used to remove the useless interference information in the step state and the abnormal data generated during the planning, which lays the foundation for the accurate path planning.

2 Based on the above results, the multi-objective optimisation model of path selection is constructed, and the Nash negotiation axiom is used to solve the model to complete the path planning of self-driving tour.

3 Experimental verification. Taking the abnormal data clearance rate, planning average delay, planning cost and planning efficiency as experimental indicators, the proposed method is compared with the methods in Wei and Jin (2019), Feng and Yang (2019), and Li and Hu (2018).

Through the above scheme, the accurate and rapid planning of self-driving travel path can be realised.

2 Path planning method of self-driving tour

2.1 Abnormal data removal based on collaborative edge computing

In the process of data collection, noise is unavoidable. In the process of vehicle walking, the speed and line are constantly changing. The measured acceleration curve has obvious oscillation peak, wave trough and zero axis, which makes the operation of gait detection more difficult and reduces the accuracy.

Collaborative edge computing is one of the most important algorithms in the field of information processing and data analysis. It mainly uses computer efficient and fast edge computing methods (Qi et al., 2019; Wu and Wang, 2016). The ordered long sequence can be transformed into the ordered long sequence by the frequency domain off the cooperative edge processing according to the cooperative edge calculation, and effectively reduce the calculation amount of the algorithm, so it has been widely used (Liu and Wang, 2017).

Three axis acceleration is defined as a three-dimensional data a_x, a_y, a_z. The time dimension is t, and the signal of each acceleration is represented as a three-dimensional vector $a(a_x, a_y, a_z)$. It represents the acceleration and time of different coordinate stations respectively. Combined with FFT formula processing, the forward and inverse forms of the formula are as follows:

$$X_k = \sum_{n=0}^{N-1} x_n * e^{-i2\pi kn/N} \tag{1}$$

$$X_n = \frac{1}{N} \sum_{k=0}^{N-1} x_k * e^{-i2\pi kn/N} \tag{2}$$

where N represents the size of the Fourier transform window, k represents the acceleration period, and $e^{(-i2\pi)}$ represents the Fourier transform vector.

The following formula defines the FFT processing formula of triaxial acceleration, as shown in formula (3):

$$D(f) = f\left(vec(x, y, z, t+1)\right) \tag{3}$$

where vec(.) is the acceleration response function, f is the FFT processing parameter.

Fourier transform is used to deal with noise. In the process of fast Fourier transform, the data will have a change amplitude. The larger the amplitude is, the greater the change of data is. The frequency of walking and the filtering range of acceleration are calculated by the amplitude (Zho et al., 2018; Jin et al., 2018).

When the data is filtered, arithmetic moving average processing begins. α_k represents the acceleration in time k, and the corresponding sliding window is set by the change of acceleration value.

The average value of N accelerations a_k^s can be expressed as follows:

$$a_k^s = \sum_{i=0}^{N-1} a_{k-i} / N \tag{4}$$

Step detection plays an important role in the whole research process. In the process of self-driving tour, people will enjoy the surrounding scenery on foot. According to the movement data collected by smart phones, it is necessary to consider the natural swing of human body and the walking speed that pedestrians may change according to the actual situation. Therefore, the above factors cause the oscillation of the signal around the zero axis, resulting in false peak value and false valley value. The correct transition state and wrong transition state are shown in Figure 1 and Figure 2 respectively.

Figure 1 Step correct transition state

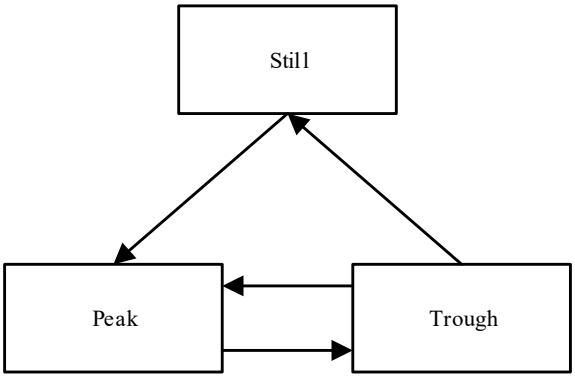

Figure 2 Step error transition state

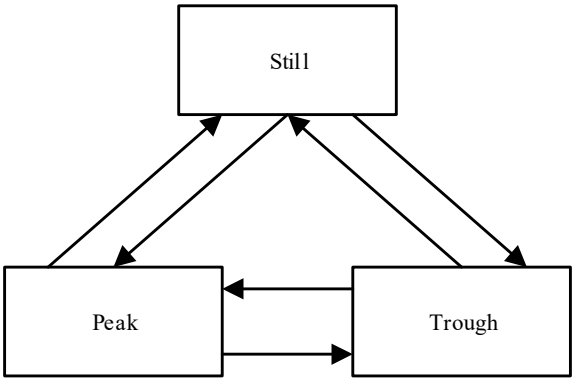

Static stands for standing at rest, peak represents the increase of speed reaches the optimal value, and the trough represents the state when the speed decreases to 0. The state of walking can be determined according to the state threshold (Ren et al., 2018). The state threshold setting can be divided into three different forms as follows:

1 quiescent threshold T_s

2 peak threshold T_p

3 low threshold $T_{l.}$

The threshold can determine the state of acceleration. Set three initial state thresholds as $T_{s,k}$, $T_{p,k}$, $T_{l,k}$ respectively represent the state threshold in the gait period K (Liu et al., 2016; Li et al., 2016), and the specific formula can be expressed as follows:

$$\begin{cases} T_{s,k} = R_{0,k} + T_s \\ T_{p,k} = R_{0,k} + T_p \\ T_{l,k} = R_{0,k} + T_l \end{cases} \tag{5}$$

where $R_{0,k}$ represent the gait period.

Because of the difference of acceleration, the acceleration zero axis moves up and down.

The specific calculation formula of the gait period $R_{0,k}$ is given below:

$$b_i = \begin{cases} \dfrac{\left(a_{i-1,\min} + a_{t,\max}\right)}{2}, & \text{state = peak value} \\ \dfrac{\left(a_{i-1,\max} + a_{t,\min}\right)}{2}, & \text{state = peak base} \\ \dfrac{\sum_{j=1}^{m} a_{i,j}}{m}, & \text{state = static} \end{cases} \tag{6}$$

In addition to threshold setting, it also sets the longest duration and the shortest duration of a gait state. The main purpose of setting the minimum duration is to delete the short-term noise, and the main purpose of setting the maximum duration is to reduce the error rate of step count and filter out the long-lasting useless data (Yu et al., 2019). Assuming that the current acceleration data does not cross the state boundary value, and the duration is legal, then the state is transferred to the next stage through the state diagram; if the data is illegal, the state is set as static state. The main reason for this is the noise. The sliding window for processing data is set as follows:

$$window - size = \Delta T * f \tag{7}$$

where *size* is the size of the *window* and ΔT is the periodic change.

Through a more feasible method, the relationship between acceleration and vehicle driving is calculated (Wang, 2018; Xu et al., 2016), and the specific calculation formula is as follows:

$$l = h * \sqrt[4]{a_{\max} - a_{\min}} \tag{8}$$

where h is the distance traveled.

The relationship between average acceleration and vehicle driving is shown in formula (9)

$$l = h * \sqrt[3]{\frac{\sum_{i=1}^{N} |a_i|}{N}} \tag{9}$$

Relevant experts improve the above formula:

$$l = h * \frac{\dfrac{\sum_{i=1}^{N} |a_i|}{N} - a_{\min}}{a_{\max} - a_{\min}} \tag{10}$$

The distance traveled by users of self-driving tour can be calculated by vehicle speed, that is, the cumulative sum of all effective vehicle travel speeds (Cao and Yu, 2018). The specific calculation formula is as follows:

$$D_{distance} = \sum_{i=1}^{N} l_i \tag{11}$$

To sum up, according to the influence of noise, the collaborative edge calculation method can effectively filter out the abnormal data generated in the process of self-driving tour.

$$\begin{bmatrix} E_x \\ E_y \\ E_z \end{bmatrix} = D_{distance} \begin{bmatrix} E_x^s \\ E_y^s \\ E_z^s \end{bmatrix} \tag{12}$$

where E_x, E_y, E_z is the result of 3D noise filtering.

2.2 Construction of multi-objective optimisation model

On the basis of clearing abnormal data in Section 2.1, a multi-objective optimisation model is established (Lu and Hu, 2017). The diversity of parameters in the multi-objective optimisation model can improve the effectiveness of path planning. Game theory is a very large theoretical system, in which there are different types of game theory. Cooperative game theory plays a very important role in the whole system of game theory, and it is also a very complex concept.

Assuming that there are N players in the game (Yan et al., 2019; Shi et al., 2019), the strategy combination composed of the strategies selected by each player can be expressed in the following form:

$$s = \left\{ s_1^*, s_2^*, s_3^*, \ldots, s_N^* \right\} \tag{13}$$

The s in formula (13) contains a strategy group for each player i, that is:

$$s = \left\{ s_1^*, s_2^*, s_{i-1}^*, s_i^*, s_{i+1}^*, \ldots, s_N^* \right\} \tag{14}$$

where, formula (14) represents the optimal strategy combination, and the constraints of formula (15) need to be satisfied:

$$u_i \left\{ s_1^*, s_2^*, s_3^*, \cdots, s_N^* \right\} = u_i \left\{ s_1^*, s_2^*, s_{i-1}^*, s_i^*, s_{i+1}^*, s_N^* \right\} \tag{15}$$

Formula (15) represents that the game process has reached the equilibrium state, and the corresponding strategy combination $s = \left\{ s_1^*, s_2^*, s_3^*, \ldots, s_N^* \right\}$ is the Nash equilibrium solution.

Cooperative game occupies a very important position in the whole game theory system (Yuan et al., 2019), and it is also a very complex concept. Cooperative game is actually in the process of the game, before players play, in order to achieve the ultimate common goal of negotiation, and at the same time take a consistent action plan.

From Nash's point of view, the negotiation between players in cooperative games focuses on two aspects, namely:

1 when the consensus agreement between the authorities cannot be reached, the players can obtain special benefits

2 revenue is mainly used to represent the set of feasible payments.

Combined with the above analysis, it is clear that the key QoS parameters of user experience quality index are four common parameters in the whole network system.

Combined with the correlation analysis in Section 2.1, the objective function of user experience quality level evaluation of self-driving travel path planning method is established. Matter element is used to describe the evaluation level of user experience quality index. The different characteristics of the evaluation level are the above four general parameters (Xu et al., 2019; Zhang et al., 2020), which are respectively expressed as C_1, C_2, C_3, C_4, the unit of magnitude value corresponding to the feature is the value range of corresponding parameter, which is expressed as C_1, C_2, C_3, C_4. Therefore, the matter-element of user experience quality evaluation level in the self-driving travel path planning method can be expressed in the following forms:

$$R_j = \left(N_j, C_i, V_{ji}\right) = \begin{cases} N_j C_1 \left\langle a_{j1}, b_{j1} \right\rangle \\ C_2 \left\langle a_{j2}, b_{j2} \right\rangle \\ C_3 \left\langle a_{j3}, b_{j3} \right\rangle \\ C_4 \left\langle a_{j4}, b_{j4} \right\rangle \end{cases} \tag{16}$$

where R_j stands for the matter element of user experience quality evaluation level. N_j represents the user experience quality evaluation grade series; the following five user experience quality rating levels (Shen et al., 2017; Xing et al., 2019) recommended by ITU are selected as follows:

1 excellent

2 good

3 medium

4 bad

5 inferior.

The quantitative values of the above five grades are 5, 4, 3, 2, 1. C_i represents the characteristics of different matter elements.

Combined with matter-element analysis theory, the i^{th} feature C_i of user experience quality evaluation level of candidate path P can be obtained and the correlation degree of any matter element R_j is calculated as follows:

$$k_j\left(V_i\right) = \begin{cases} -\dfrac{\rho\left(V_i, V_{ji}\right)}{d}, & V_i \in V_{ji} \\ \dfrac{\left(V_i, V_{ji}\right)}{\left(\rho\left(V_i, V_{ei}\right) - \rho\left(V_i, V_{ji}\right)\right)}, & V_i \in \nexists V_{ji} \end{cases} \tag{17}$$

where $k_j(V_i)$ represents the correlation degree between the i^{th} feature of the matter element to be evaluated and any matter-element; d represents the membrane corresponding to the value range of characteristic C_i calculated according to the interval modeling formula represents the feature, namely:

$$d = \begin{cases} \left|V_{ji}\right| \\ \left|a_{ji} - b_{ji}\right| \end{cases} \tag{18}$$

Set $\rho(V_i, V_{ji})$ represents the distance between the quantity value and the corresponding interval, which can be expressed in the following form:

$$\rho\left(V_i, V_{ji}\right) = \left|V_i - \left(a_{ji} + b_{ji}\right)\right| - \left(b_{ji} - a_{ji}\right)/2 \tag{19}$$

$$\rho\left(V_i, V_{ei}\right) = \left|V_i - \left(a_{ei} + b_{bi}\right)\right| - \left(b_{ei} - a_{ei}\right)/2 \tag{20}$$

According to the above formula, the comprehensive correlation degree of multiple features of the user experience quality evaluation level of the candidate path with respect to any matter-element is as follows:

$$K_j(P) = \sum\nolimits_{i=1}^{T} \omega_i k_i\left(V_i\right) \tag{21}$$

where T represents the total number of characteristic indexes; ω_i represents the weight of different features of user experience quality evaluation. Because the influence of different features on matter-element is different, different weight should be given to its importance. The weight is calculated by fuzzy analytic hierarchy process. For the candidate path, The larger the value of $K_j(P)$, the more consistent with the corresponding user experience quality evaluation level. From the perspective of different users, the user experience quality of the candidate path is given by formula (21), and the grade objective function is evaluated:

$$F_{QoE}(P) = \max_{k=1}\left(K_j(P)\right) \tag{22}$$

In terms of network performance, if the whole network has a high channel capacity, users can get higher data transmission rate. At the same time, the system throughput and system capacity also be greatly improved. The capacity of different channel links can be expressed as follows:

$$W - W\log_2\left(1 + \frac{G_{s,r}^2 E_b R_s}{N_0 + \sum_{t\in\lambda} G_{t,r}^2 E_b R_t}\right) \tag{23}$$

where $G_{s,r}^2$ represents the link loss.

The channel capacity objective function corresponding to the candidate path is constructed as follows:

$$F_{capacity}(P) = \max_{k=1}\left(W\left(P_k\right)\right) \tag{24}$$

where P_k represents the channel capacity state parameter.

If S represents the set of candidate paths, then the multi-objective optimisation model is as follows:

$$P* = \begin{cases} \max F(P) = \left\{F_{QoE}(P), F_{capacity}(P)\right\} \\ \text{s.t. } P \in S \end{cases} \tag{25}$$

2.3 Multi objective optimisation model solution

Through the content analysis of the above sections, the current situation is the basis for the players to carry out cooperative negotiation, and all players can not give in, so the benefit effect and the final negotiation result will be affected to varying degrees. In the process of practical application, the players are not completely antagonistic, and the gains and losses between them can not be zero. Therefore, the current situation mainly refers to the benefits obtained by the players by choosing conservative strategies in the non cooperative game (Zeng et al., 2019):

$$sta_i = \left\{ \max_{X \in S_1} \max_{Y \in S_2} E_i(X, Y) \right\} \tag{26}$$

where S_1, S_2 represents the mixed strategy set of two players participating in cooperative negotiation, and the two strategies need to satisfy the following constraints:

$$S_1 = \left\{ X \middle| x_i \geq 0, \quad \sum_{i=1}^{n} x_i = 1 \right\} \tag{27}$$

$$S_2 = \left\{ Y \middle| y_i \geq 0, \quad \sum_{i=1}^{n} y_i = 1 \right\} \tag{28}$$

Combined with the above algorithm analysis, the basic steps of self-driving tour path planning can be described as follows:

1 the network obtains the detailed location information of mobile station and relay station by initialising parameter set

2 when the mobile station is connected to the network to form service data, the output transmission is needed

3 the objective function of user experience quality rating grade of candidate path is established to meet the needs of users

4 the objective function of network channel capacity on the candidate path is constructed

5 the two objective functions in step 3 and step 4 are simulated as players in the game process, and the candidate path is set as the action strategy of players;

6 in the process of the game, the two sides get the negotiation cooperation shop, namely, Nash negotiation solution; assuming that the negotiation cooperation shop is not found, both sides of the game need to choose the next action strategy and return to step (5)

7 the best transmission path is selected by the action strategy of Nash negotiation solution

8 assuming that the selected new path is not the initial path, the new path is set as the transmission path of the mobile base station

9 end.

The solution flow of multi-objective optimisation model is shown in Figure 3.

Figure 3 Solution flow of multi-objective optimisation model

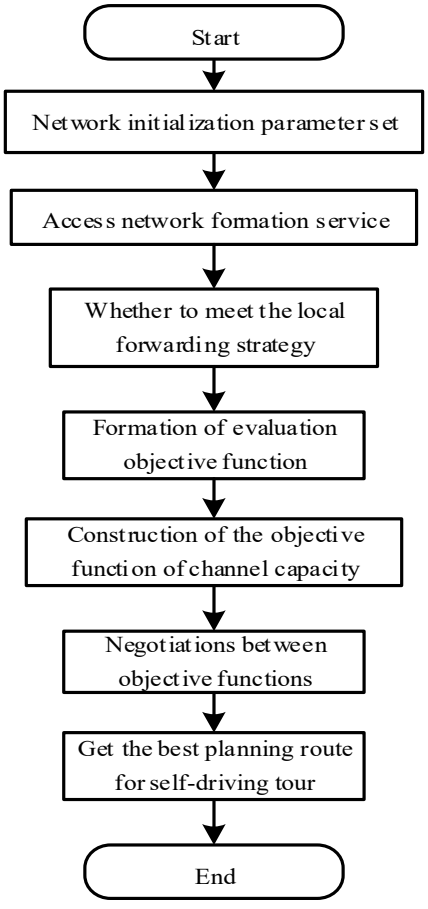

Based on the above analysis, the multi-objective optimisation model is solved by combining Nash negotiation axiom in game theory to obtain the best self-driving path planning.

In order to improve the accuracy of self-driving travel path planning, collaborative edge computing is used to clear abnormal data. On this basis, the multi-objective optimisation model of path planning is constructed, and the Nash negotiation axiom is used to solve the multi-objective optimisation model, so as to realise the accurate and rapid path planning of self-driving tour.

3 Simulation experiment

In order to verify the comprehensive effectiveness of the proposed self-driving travel path planning method based on collaborative edge computing, comparative experiments are carried out. The experimental environment is: the processor is Intel(R)Core(TM)i7-4590CPU, 3.30 GHz, 16g memory and 64 bit windows7 operating system. The experimental data is from Oracle relational database, in which the size of

collected data is 5GB. In order to improve the accuracy of the experimental results, the bilateral filtering method is used to filter the experimental data.

Under the above experimental environment, the overall experimental scheme is set as follows: Taking the abnormal data clearance rate, planning average delay, planning cost and planning efficiency as the experimental comparison indexes, the proposed method is compared with the methods in Wei and Jin (2019), Feng and Yang (2019) and Li and Hu (2018).

1 Abnormal data clearance rate: path planning is completed by processing related data, and the existence of abnormal data reduces the accuracy of path planning. Therefore, setting the abnormal data clearance rate as the comparison index, the higher the abnormal data clearance rate is, the more accurate the path planning result will be.

2 Average planning delay: the average planning delay refers to the asynchronous phenomenon in the planning process. The longer the delay, the worse the effectiveness of the planning method.

3 Planning cost: planning cost refers to the cost of planning a path. The lower the planning cost, the higher the effectiveness of the method.

4 Planning efficiency: planning efficiency refers to the efficiency of different planning methods for the same self-driving tour site. The higher the planning efficiency, the higher the effectiveness of the method.

3.1 Comparison of abnormal data clearance rate

In the process of self-driving travel path planning, due to the existence of abnormal data, the planning results are not accurate, so in the early stage of the experiment, it is necessary to clear the abnormal data. The results of the four methods are shown in Table 1.

Table 1 Abnormal data clearance rate of different methods

Number of test samples / (piece)	*Abnormal data clearance rate / (%)*			
	The proposed method	*Method of Wei and Jin (2019)*	*Method of Feng and Yang (2019)*	*Method of Li and Hu (2018)*
1,500	98.21	54.14	56.17	96.52
2,000	99.36	84.51	45.61	56.45
2,500	97.85	48.51	89.74	63.12
3,000	96.54	62.13	48.97	85.96
3,500	98.41	85.41	56.31	87.40
4,000	97.69	51.40	78.91	52.63
4,500	98.81	57.45	64.59	96.51
5,000	99.36	74.89	78.96	41.61
5,500	97.83	45.61	56.44	48.51
6,000	96.21	89.67	59.74	74.59
6,500	98.36	56.32	78.94	89.41
7,000	98.14	61.52	89.64	84.23
7,500	99.74	45.61	56.41	45.17

It can be seen from the experimental results in Table 1 that the anomaly removal rate of the proposed method is higher than that of the three reference comparison methods, and the highest removal rate can reach 99.74%, which can effectively improve the accuracy of self-driving travel path planning.

3.2 Comparison of planning average delay

The planning average delay comparison results of the four methods are shown in Figure 4.

Figure 4 Comparison results of average delay of path planning

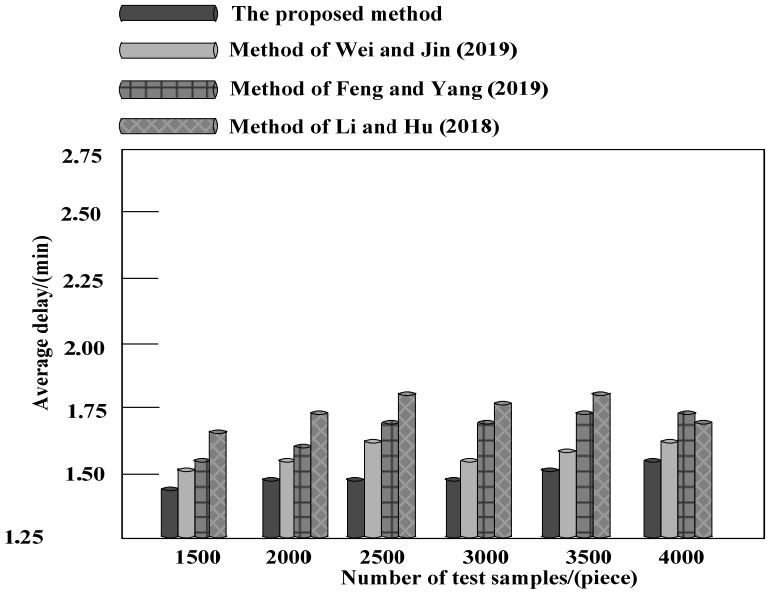

Analysing the experimental data in Figure 4c it can be seen that with the continuous increase of the number of test samples, the average experiments of various path planning methods are also increasing. However, compared with the other three methods, the average delay of the proposed method is significantly lower. The main reason is that the proposed method eliminates the abnormal data to effectively reduce the path planning delay.

3.3 Comparison of planning cost

The cost comparison results of the four methods are shown in Table 2.

Analysis of the experimental data in the above table shows that the planning cost of various path planning methods is also changing with the continuous increase of running time. Because the proposed method can effectively remove abnormal data, the planning cost of the proposed method is significantly lower than that of the other three methods. The other three methods do not clear the abnormal data in detail, which makes the planning cost increase obviously.

Table 2 Path planning cost of different methods

Running time / (min)	*Path planning cost / (10,000 yuan)*			
	The proposed method	*Method of Wei and Jin (2019)*	*Method of Feng and Yang (2019)*	*Method of Li and Hu (2018)*
30	0.858	0.908	0.948	1.039
45	0.877	0.935	0.975	1.078
60	0.904	0.971	1.024	1.145
75	0.932	1.032	1.145	1.182
90	0.951	1.073	1.172	1.233
105	0.985	1.125	1.231	1.280
120	1.025	1.165	1.284	1.367
135	1.032	1.202	1.322	1.419
150	1.051	1.240	1.372	1.475
165	1.086	1.272	1.410	1.556
180	1.109	1.318	1.463	1.598
195	1.135	1.367	1.495	1.642
210	1.152	1.402	1.532	1.679
225	1.181	1.462	1.589	1.785

3.4 Comparison of planning efficiency

The comparison results of the four methods are shown in Table 3.

Table 3 Planning efficiency of different methods

Number of experiments / (times)	*Planning efficiency / (%)*			
	The proposed method	*Method of Wei and Jin (2019)*	*Method of Feng and Yang (2019)*	*Method of Li and Hu (2018)*
150	98.21	96.85	94.85	87.85
200	96.29	97.36	93.14	86.36
250	97.36	94.52	90.25	85.41
300	98.84	93.14	89.52	84.14
350	96.73	92.52	87.25	83.85
400	97.52	91.22	86.20	84.96
450	99.14	94.96	85.96	82.77
500	98.25	93.25	88.24	81.85
550	97.85	92.25	87.85	83.25
600	96.22	90.15	89.14	82.52
650	98.14	91.52	90.84	84.12
700	99.96	92.25	87.21	83.00
750	99.12	93.62	86.10	82.14

Analysis of the above experimental data shows that the proposed method after the exception data removal, the execution efficiency has been very effectively improved, but the other methods do not clear the abnormal data, which makes the execution efficiency of the whole method show an obvious downward trend.

The experimental process takes the abnormal data clearance rate, planning average delay, planning cost and planning efficiency as the experimental comparison indexes, which fully proves the effectiveness of the proposed self-driving travel path planning method from multiple angles. The proposed planning method can effectively remove abnormal data, shorten planning delay and reduce planning cost, and can meet the requirements of efficient planning.

4 Conclusions

There are a lot of abnormal data in the traditional methods, which lead to the problems of low planning efficiency and high cost in the final planning results. The following conclusions are proved in theory and experiment. This method has a high rate of abnormal data removal and planning efficiency. Specifically, compared with the method based on road network, the removal rate of abnormal data is significantly improved, with the highest removal rate of 99.74%; compared with the method based on RFID technology, the planning efficiency is greatly improved, and the maximum planning efficiency is 99.96%. Therefore, the proposed planning method based on collaborative edge computing can better meet the requirements of self-driving travel path planning. In the follow-up research process, the research scope will be expanded and the applicability of the proposed method will be enhanced.

Acknowledgements

This work was supported by Tourism management team of the central government supports special projects for local universities 2019

References

Cao, X. and Yu, A.L. (2018) 'Complete-coverage path planning algorithm of mobile robot based on belief function', *CAAI Transactions on Intelligent Systems*, Vol. 13, No. 2, pp.314–321.

Chu, J.L., Zhang, P.Y. and Chen, Y.W. (2018) 'Simulation of tourist congestion and evacuation path planning in tourist attractions', *Computer Simulation*, Vol. 35, No. 4, pp.85–88+431.

Feng, H.F. and Yang, Z.J. (2019) 'Hot passenger paths mining based on spatial-temporal similarity clustering', *Journal of Transportation Systems Engineering and Information Technology*, Vol. 19, No. 5, pp.94–100.

Jin, Z.J., Cheng, G., Guo, F. and Wei, H.R. (2018) 'Optimal path planning algorithm for coal mine search and rescue robots', *Industrial and Mine Automation*, Vol. 44, No. 10, pp.24–28.

Li, X.Y. and Hu, R.X. (2018) 'High speed road network path accurate identification technology based on RFID technology', *GongluJiaoTongKeJI*, Vol. 14, No. 10, pp.292–294.

Li, Z.Y., Cheng, L.X., Wang, Z.Z., Li, C., Xu, J.Z. and Xiao, G.X. (2016) 'Distribution automation terminal layout planning method', *Power Grid Technology*, Vol. 40, No. 4, pp.1271–1276.

Liu, N.N. and Wang, H.W. (2017) 'Path planning of mobile robot based on the improved grey wolf optimization algorithm', *Electrical Measurement & Instrumentation*, Vol. 57, No. 1, pp.76–83+98.

Liu, X.L., Jiang, L., Jin, Z.F. and Guo, C. (2016) 'Path planning of mobile robot based on grid method environment modeling in unstructured environment', *Machine Tool and Hydraulics*, Vol. 44, No. 17, pp.1–7.

Lu, C. and Hu, J.G. (2017) 'Path planning and tracking control in the position servo control system of permanent magnet synchronous motors', *Motor and Control Applications*, Vol. 44, No. 2, pp.23–27+46.

Qi, Z.G., Huang, P.F., Liu, Z.X. and Han, D. (2019) 'Research on path planning method of spatial redundant manipulator', *Journal of Automation*, Vol. 45, No. 6, pp.1103–1110.

Ren, B.Y., Wei, K. and Wu, Z.Q. (2018) 'Research progress of path planning for visual servoing of robotic manipulator', *Journal of Harbin Institute of Technology*, Vol. 50, No. 1, pp.7–16.

Shen, J., Hong, L., Ji, B.J. and Ling, C. (2017) 'Intersecting pipe path planning of arc welding robot system', *Mechanical Design and Research*, Vol. 33, No. 6, pp.48–51.

Shi, Q., Lv, L., Xie, J.j. and Tao, J.A. (2019) 'Low-swing vibration path planning of robot machining tool axis based on free surface directed voronoi region division algorithm', *Computer Integrated Manufacturing System*, Vol. 25, No. 5, pp.1093–1100.

Wang, Z.Z. (2018) 'Path planning for molile robot based on improved ant colony algorithm', *Machinery Design & Manufacture*, Vol. 23, No. 1, pp.248–250.

Wei, Y.L. and Jin, W.Y. (2019) 'Intelligent vehicle path planning based on neural network Q-learning algorithm', *Fire Control & Command Control*, Vol. 44, No. 2, pp.48–51.

Wu, F. and Wang, X.Z. (2016) 'Research on intelligent monitoring and path planning and design of picking robots', *Agricultural Mechanization Research*, Vol. 38, No. 7, pp.40–44.

Xing, P.X., Li, Q., Wei, W. et al. (2019) 'Application of AGV path planning based on improved A * algorithm in intelligent warehousing', *Information Technology*, Vol. 43, No. 5, pp.138–141.

Xu, X.G., Hu, N., Xu, Y.X. and Wang, L. (2016) 'Application of improved firefly algorithm in path planning', *Journal of Electronic Measurement and Instrument*, Vol. 30, No. 11, pp.1735–1742.

Xu, Z., Hu, J.W., Ma, Y.H., Wang, M. and Zhao, C.H. (2019) 'Research on UAV collision avoidance path planning algorithm', *Journal of Northwestern Polytechnical University*, Vol. 37, No. 1, pp.100–106.

Yan, X., Gao, J.W. and Guan, C. (2019) 'Path planning of wave glider based on mode transformation ant colony algorithm', *Computer Engineering and Applications*, Vol. 55, No. 9, pp.100–106+229.

Yu, X.Y., Lu, L., Zhu, Y.C. and Ou, L.L. (2019) 'Automated parking lot scheduling method based on heuristic dynamic programming', *High Technology Communication*, Vol. 29, No. 4, pp.352–361.

Yuan, S., Xing, J.Y., Yao, X., Luan, F.J. and Zhao, S.B. (2019) 'Path planning for nanomanipulators based on probability distribution intervals', *Control Theory and Applications*, Vol. 36, No. 1, pp.129–142.

Zeng, P., Wang, H.L. and Wang, Y.L. (2019) 'An driverless dynamic path planning algorithm based on Vanet', *Computer Engineering and Science*, Vol. 41, No. 11, pp.2055–2062.

Zhang, Y.X., Wang, Y.Q., Li, S. et al. (2020) 'Global path planning for auv based on charts and the improved particle swarm optimization algorithm', *Robot*, Vol. 42, No. 1, pp.120–128.

Zho, W.J., Yu, H.W., Zhou, W.X. and Wang, W. (2018) 'Research on robot path planning of automated stamping production line', *Foundry Technology*, Vol. 39, No. 8, pp.1754–1759+1767.